

Supporting Information

Pressure-Stimulus-Responsive Behaviors of Core–Shell InP/ZnSe Nanocrystals: Remarkable Piezochromic Luminescence and Structure Assembly

*Hao Liu,^{a, b} Yixuan Wang,^a Xinyi Yang,^{*a} Xiaohui Zhao,^a Kai Wang,^a Min Wu,^a Xiaobing Zuo,^c
Wenge Yang,^d Yongming Sui,^{*a} and Bo Zou^{*a}*

^a State Key Laboratory of Superhard Materials, College of Physics, Jilin University,
Changchun 130012, China

^b School of Physics and Electronic Engineering, Xinxiang University, Xinxiang 453003,
China

^c X-ray Science Division, Advanced Photon Source, Argonne National Laboratory, Lemont,
IL 60439, United States

^d Center for High Pressure Science and Technology Advanced Research (HPSTAR), Beijing
100094, China

*Corresponding authors: yangxinyi@jlu.edu.cn; suiym@jlu.edu.cn; zoubo@jlu.edu.cn

EXPERIMENTAL DETAILS

Sample preparation and high-pressure generation.

Synthesis of InP nanocrystals (NCs): InP NCs were synthesized based on the method described in the literature.¹ In a typical synthesis, 0.45 mmol InCl₃ and 2.2 mmol ZnCl₂ were mixed with 5 mL oleylamine in a 50 mL three-neck flask. The reaction mixture was degassed under vacuum at 120 °C for 30 min and then heated to 190 °C. Next, 0.45 mL (1.6 mmol) tris(diethylamino)phosphine was quickly injected into the reaction flask, and the solution was continuously degassed and purged with nitrogen for 30 min. Afterward, the reaction solution was cooled to room temperature. The InP NCs were precipitated using acetone and centrifuged at 10000 rpm. The precipitate was re-dispersed in toluene and precipitated with acetone. This process was repeated a minimum of three times and the precipitation dried under vacuum for 1 h at 50 °C to get InP NCs powder.

Synthesis of Core-Shell InP/ZnSe NCs: An InP NCs synthesis is performed at 190 °C. Instead of cooling down the temperature, at 20 min: slow injection of 1 mL of saturated TOP-Se (2.2 M). At 60 min: temperature is increased from 190 to 210 °C. At 120 min: slow injection of 1 g of Zn(stearate)₂ in 4 mL of octadecene (ODE). Temperature is increased from 210 to 220 °C. At 150 min: injection of 0.7 mL of stoichiometric TOP-Se. Temperature is increased from 220 to 240 °C. At 180 min: slow injection of 0.5 g of Zn(stearate)₂ in 2 mL of ODE. Temperature is increased from 240 to 280 °C. At 210 min: injection of 0.7 mL of stoichiometric TOP-Se. Temperature is increased from 280 to 320 °C. At 240 min: slow injection of 0.5 g of Zn(stearate)₂ in 2 mL of ODE. At 270 min: end of reaction. At the end of the reaction, the temperature is cooled down. The washing and drying process was the same as that described for InP NCs.

In situ high-pressure measurements: All *in-situ* high-pressure experiments were implemented using Mao-Bell-type² symmetric diamond anvil cell (DAC) apparatus furnished with a pair of 400 μm culet diamonds (for pressures up to 40 GPa)³ at room

temperature. A T301 stainless-steel gasket was pre-indented from a thickness of 250 μm to ~ 40 μm , and a center hole at 130 μm in diameter was drilled to serve as the sample chamber. The InP/ZnSe powder was loaded into the DAC chamber together with a ruby ball and silicon oil (150 cst, Aldrich). The actual pressure was measured using the standard ruby fluorescence technique.⁴ The silicon oil was utilized as the pressure-transmitting medium to provide a hydrostatic environment.⁵ Figure S1 shows a schematic demonstration of the sample-loading and stress distribution.

In situ photoluminescence (PL) and absorption micrographs of the samples were obtained using a camera (Canon Eos 5D mark II) equipped on a microscope (Ecclipse TI-U, Nikon). The camera can record the photographs under the same conditions including exposure time and intensity. A semiconductor laser with an excitation wavelength of 355 nm was employed for all PL experiments. Note that all the parameters are fixed completely over each high-pressure PL experiment to avoid the effects of different excitation laser intensities and luminous fluxes on the resulting PL intensity. Meanwhile, the *in-situ* high-pressure absorption spectra were recorded with an optical fiber spectrometer (Ocean Optics, QE65000) using a deuterium-halogen light source.

In situ angle-dispersive X-ray diffraction (ADXRD) patterns of samples under high pressure were recorded at beamline 15U1, Shanghai Synchrotron Radiation Facility (SSRF). Both of the beamline stations at SSRF exploited a monochromatic wavelength of 0.6199 \AA . CeO_2 was utilized as the standard sample for the calibration. The Bragg diffraction rings were collected using a Mar-165 CCD detector with an average acquisition time of 30 s for each pressure and then were integrated on the basis of the Dioptas program, yielding 1D intensity versus diffraction angle 2-theta patterns.

In situ small-angle synchrotron X-ray scattering (SAXS) patterns of samples under high pressure were collected at beamline 12-ID-B at the Advanced Photon Source. The monochromatic X-ray radiation of wavelength was $\lambda = 0.4859$ \AA , and X-ray energy was 13.3 keV. The 2D scattering patterns were radially integrated to obtain

the data of 1D intensity versus q plot, where $q = 4\pi\lambda^{-1} \sin(\theta)$. The d spacing of the lattice constant of the symmetric structure can be calculated by fitting the Bragg peaks in the XRD spectrum, where $d = \lambda/(2\sin \theta) = 2\pi/q$. The lower d spacing (d) is defined as the distance between NCs.

TEM, HRTEM and Size characterization: The resulting samples were characterized by transmission electron microscopy (TEM) and high-resolution TEM performed on a JEM-2200FS with an emission gun operating at 200 kV. The TEM images were introduced into the Nano Measurer 1.2 software and the size of the nanocrystals were calibrated. The calibrated NCs size data were introduced into the originpro2017 software and fitted with Gaussian Function to obtain the average crystallite size of the NCs. The measurement data were finally represented as the mean \pm standard error (SE).

The thickness of the formed InP/ZnSe nanosheet was estimated by using the Debye-Scherrer formula⁶:

$$D = 0.89\lambda/(B\cos \theta), \quad (1)$$

where D is the thickness of the InP/ZnSe nanosheet in \AA , λ is the wavelength of scattered X-ray in \AA , θ is the diffraction angle associated with the first strongest SAXS peak and B is the angular full width at half maximum (FWHM) of the first strongest SAXS peak in rad. The first strongest SAXS peak of post-compression samples was subtracted by baseline and shown in Figure S17. The thickness was estimated by using the FWHM of the first strongest SAXS peak to the Scherrer equation. The thickness of the InP/ZnSe nanosheet is about 27.5 nm, which is equivalent to the thickness of several initial NCs.

Details of PLQY calculation: The PLQY can be calculated using the following formula:¹¹

$$\Phi = \Phi_R \frac{\int F(\lambda_{em}) A_R(\lambda_{ex}) n^2}{\int F_R(\lambda_{em}) A(\lambda_{ex}) n_R^2} \quad (2)$$

where Φ is the PLQY, $\int F(\lambda_{em})$ is the integrated intensity of emission, $A(\lambda_{ex})$ is the

percentage of light absorbed at excitation wavelength. n is the refractive index, and subscript R denotes the reference data (i.e., the PLQY at ambient pressure). n can be estimated from the Clausius-Mossotti equation and Lorentz-Lorenz equation:

$$\frac{n^2 - 1}{n^2 + 2} \cdot \frac{1}{\rho} = \frac{4\pi}{3} \cdot NA \cdot \alpha = R_{LL} \quad (3)$$

in which the density ρ can be calculated from the cell volume. R_{LL} is called the Lorentz-Lorenz constant. R_{LL} is related to polarizability α . The refractive index n at ambient pressure is 4.489.¹² By this way, the PLQY of InP/ZnSe NCs under high pressures is estimated from the integrated intensity of emission and the percentage of light absorbed at excitation wavelength, as shown in Table S1.

First-principles calculations.

Electronic band structures and structural geometrical optimization for InP were performed using projector augmented waves (PAW) method based on density functional theory as implemented in CASTEP code.^{7,8} We used the The Ceperley-Alder localdensity approximation (CA-LDA) was used to describe the exchange-correlation potential.⁹ The kinetic cutoff energy was set to 640 eV, and the Brillouin zone was sampled using the Monkhorst-Pack k-points meshes with a resolution of $2\pi \times 0.03 \text{ \AA}^{-1}$ to ensure the enthalpy converges to less than 1 meV/atom. Based on the experimental data,¹⁰ the scissor was set 0.7 eV to obtain the final band structure at various pressures.

References

- [1] Tessier, M. D.; Dupont, D.; De Nolf, K.; De Roo, J.; Hens, Z. Economic and Size-Tunable Synthesis of InP/ZnE (E = S, Se) Colloidal Quantum Dots. *Chem. Mater.* **2015**, *27*, 4893–4898.
- [2] Mao, H.; Bell, P.; Dunn, K.; Chrenko, R.; DeVries, R. Absolute Pressure Measurements and Analysis of Diamonds Subjected to Maximum Static Pressures of 1.3–1.7 Mbar. *Rev. Sci. Instrum.* **1979**, *50*, 1002–1009.

- [3] Okamura, H.; Matsunami, M.; Kitamura, R.; Ishida, S.; Ochiai, A.; Nanba, T. Infrared Studies Of electron Systems under High Pressure Using Synchrotron Radiation. *J. Phys.: Conf. Ser.* **2010**, *215*, 012051.
- [4] Mao, H. K.; Xu, J.; Bell, P. M. Calibration of the Ruby Pressure Gauge to 800 kbar under Quasi-Hydrostatic Conditions. *J. Geophys. Res.* **1986**, *91*, 4673–4676.
- [5] Klotz, S.; Chervin, J. C.; Munsch, P.; Marchand, G. Hydrostatic Limits of 11 Pressure Transmitting Media. *J. Phys. D: Appl. Phys.* **2009**, *42*, 075413.
- [6] Klug, H. P.; Alexander, L. E. *X-ray Diffraction Procedures: For Polycrystalline and Amorphous Materials*, 2nd ed.; Wiley-VCH: New York, **1974**; 992 pp, ISBN 0-471-49369-4.
- [7] Kresse, G. From Ultrasoft Pseudopotentials to the Projector Augmented-Wave Method. *Phys. Rev. B* **1999**, *59*, 1758–1775.
- [8] Segall, M. D.; Philip, J. D. L.; Probert, M. J.; Pickard, C. J.; Hasnip, P. J.; Clark, S. J.; Payne, M. C. Firstprinciples Simulation: Ideas, Illustrations and the CASTEP Code. *J. Phys.: Condens. Matter* **2002**, *14*, 2717–2744.
- [9] Ceperley, D. M.; Alder, B. J. Ground State of the Electron Gas by a Stochastic Method. *Phys. Rev. Lett.* **1980**, *45*, 566–569.
- [10] Smith, A. M.; Mohs, A. M.; Nie, S. Tuning the Optical and Electronic Properties of Colloidal Nanocrystals by Lattice Strain[J]. *Nature Nanotechnol.*, **2009**, *4*, 56–63.
- [11] Wang, Y.; Guo, S.; Luo, H.; Zhou, C.; Lin, H.; Ma, X.; Hu, Q.; Du, M.-h.; Ma, B.; Yang, W.; Lü, X., Reaching 90% Photoluminescence Quantum Yield in One-Dimensional Metal Halide $C_4N_2H_{14}PbBr_4$ by Pressure-Suppressed Nonradiative Loss. *J. Am. Chem. Soc.* **2020**, *142*, 16001–16006.
- [12] Pettit, G. D.; Turner, W. J., Refractive Index of InP. *J. Appl. Phys.* **1965**, *36*, 2081–2081.

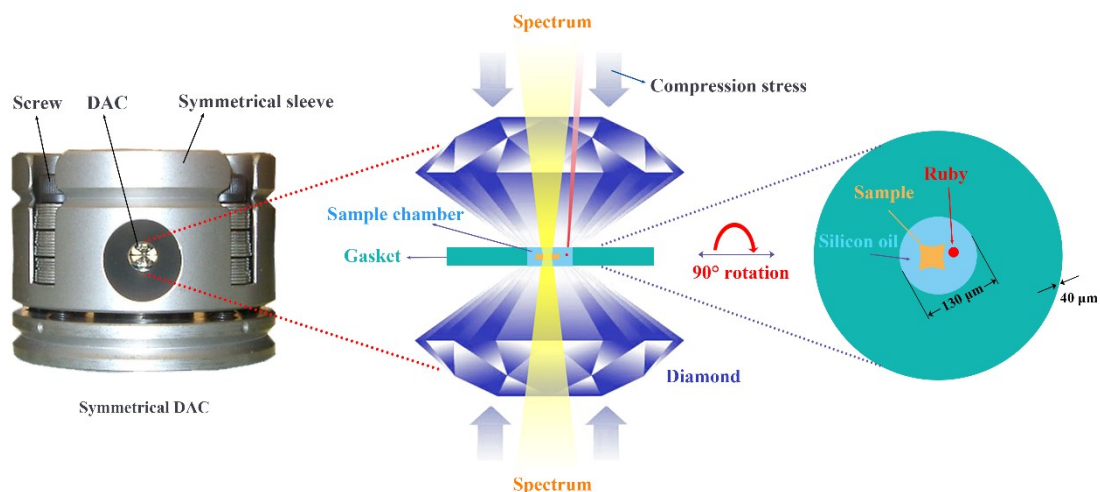


Figure S1 A schematic and detailed presentation of the DAC device. The gasket hole with 130 μm in diameter and 40 μm in thickness was drilled to serve as a sample chamber. The sample was loaded into the chamber together with a ruby ball and silicon oil.

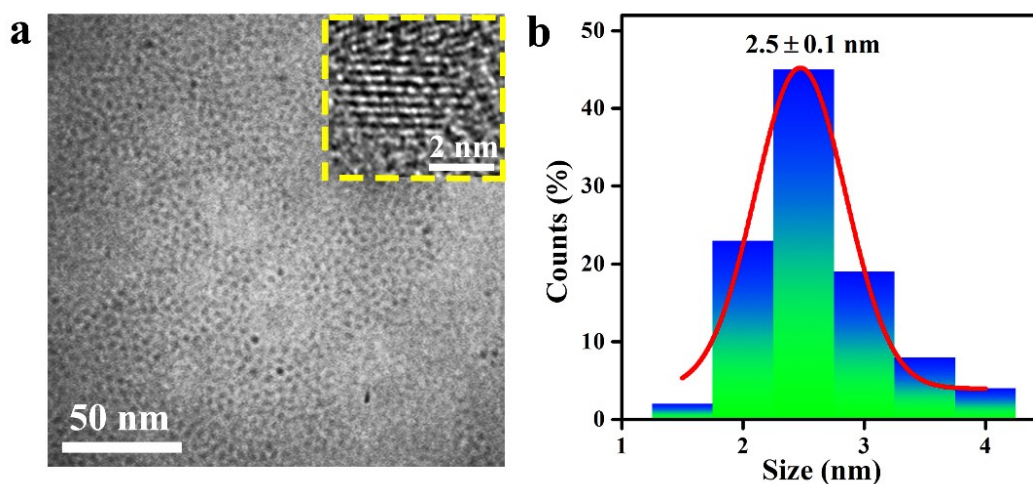


Figure S2 (a) Representative TEM image of the InP NCs. Inset: corresponding HRTEM image. (b) Corresponding size distribution histogram with Gaussian fitting. For size distribution, at least 300 NCs were analyzed, from 3 areas on the sample

TEM grid.

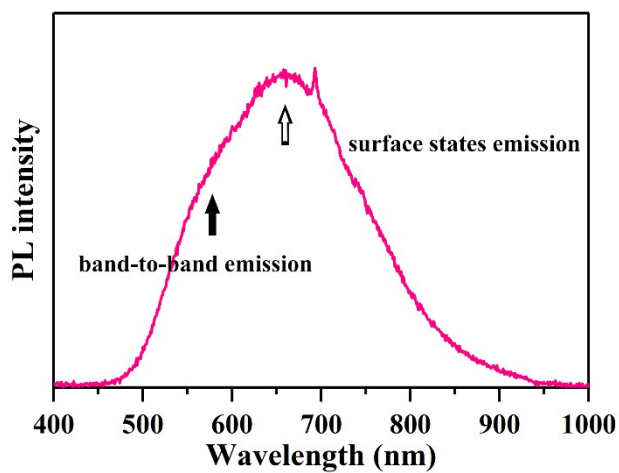


Figure S3 Ambient PL spectrum of the InP NCs. The InP NCs show weak and broad emission in the 500–900 nm region including both band-to-band and surface defect states emissions.



Figure S4 Image of the initial InP/ZnSe powder. The sample was dark brown in color under daylight.

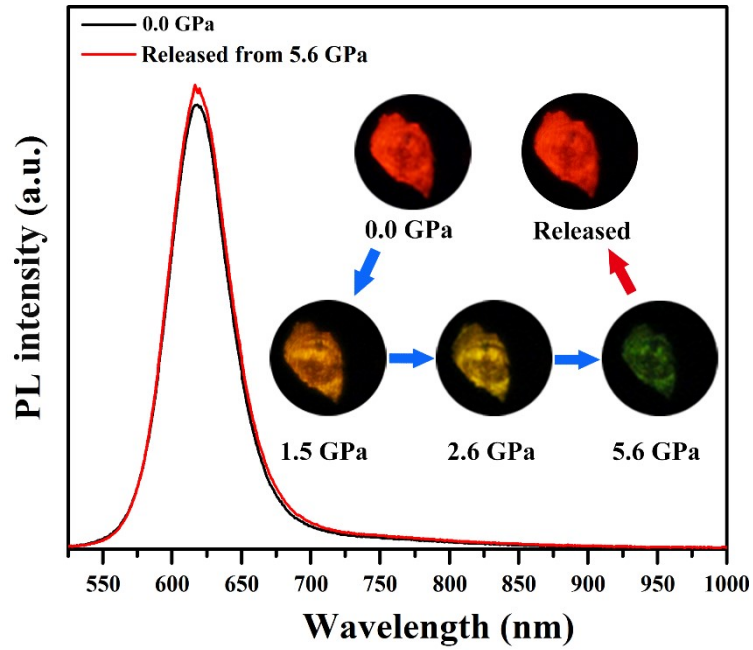


Figure S5 PL peak position and intensity comparison of the InP/ZnSe NCs before and after ~ 5.6 GPa pressurization. Inset: PL microscopic images of the InP/ZnSe NCs under UV irradiation ($\lambda_{\text{ex}} = 355$ nm) showing PL color and intensity change under high pressures. After a full pressure cycle of 0–5.6 GPa, the PL peak position and intensity returned to the initial state. This abnormal phenomenon could be reproduced in our repeated experiments.

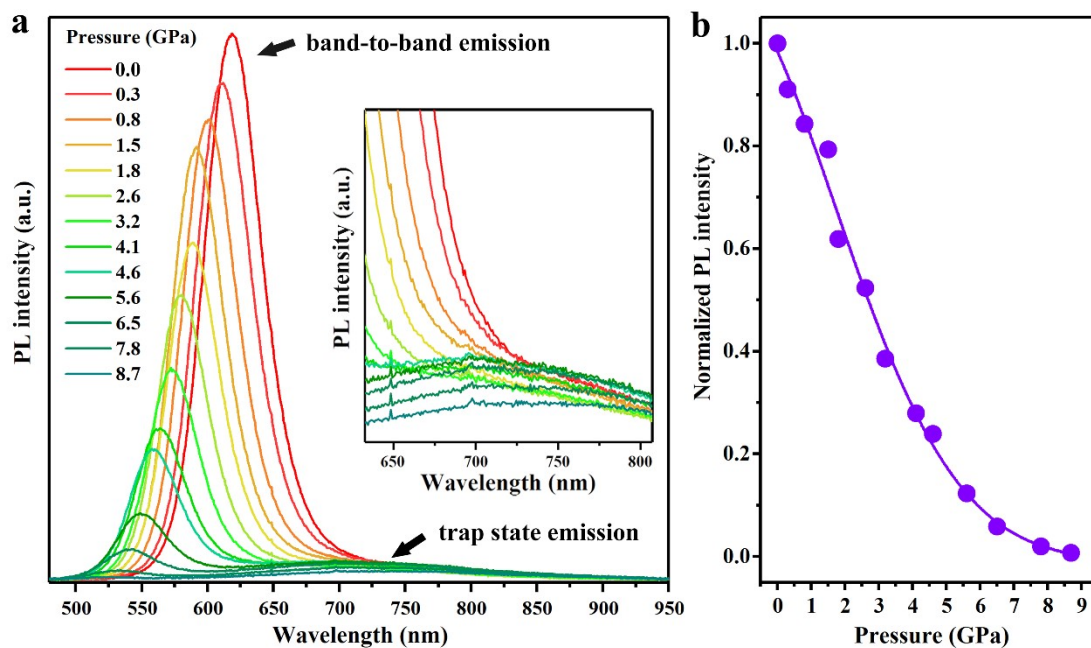


Figure S6 (a) Changes in the PL spectra of the InP/ZnSe NCs with the increase in the pressure from 0 to 8.7 GPa. With the increase in pressure, the intensity of the band-to-band emission spectrum weakened and the peak position blue-shifted until the PL completely disappeared at 8.7 GPa. The trap emission is generally less sensitive to pressure. Inset: The low-energy part of the spectra is zoomed in inset. (b) Normalized PL intensity of the InP/ZnSe NCs as a function of the pressure.

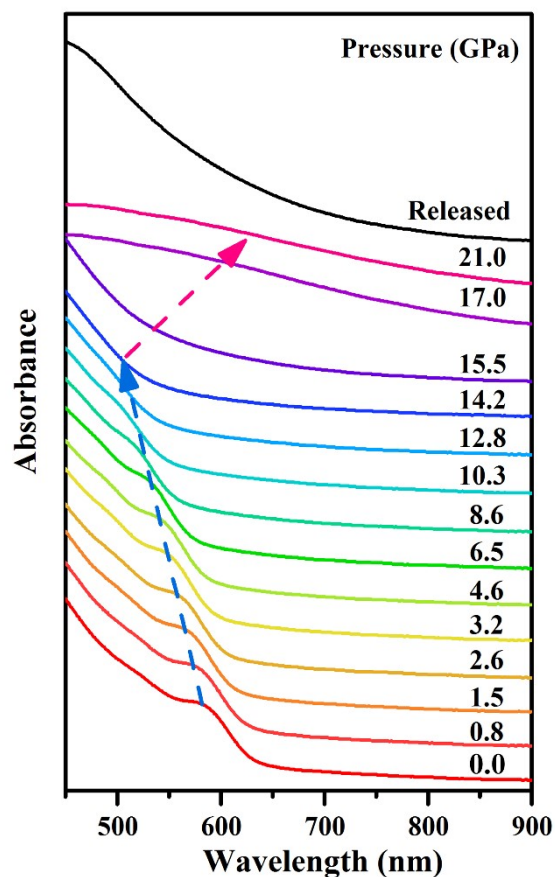


Figure S7 Absorption spectrum of the InP/ZnSe NCs as a function of the pressure. The pressure-dependent absorption spectrum of the InP/ZnSe NCs exhibited a blue-shift with the increase in the pressure from 0 to 14.2 GPa. When a considerably higher pressure (above 14.2 GPa) was applied, an abrupt red-shift was observed up to the maximum pressure study point of 21.0 GPa. When the pressure was released from 21.0 GPa, the absorption edge exhibited a red-shift in comparison with the initial that.

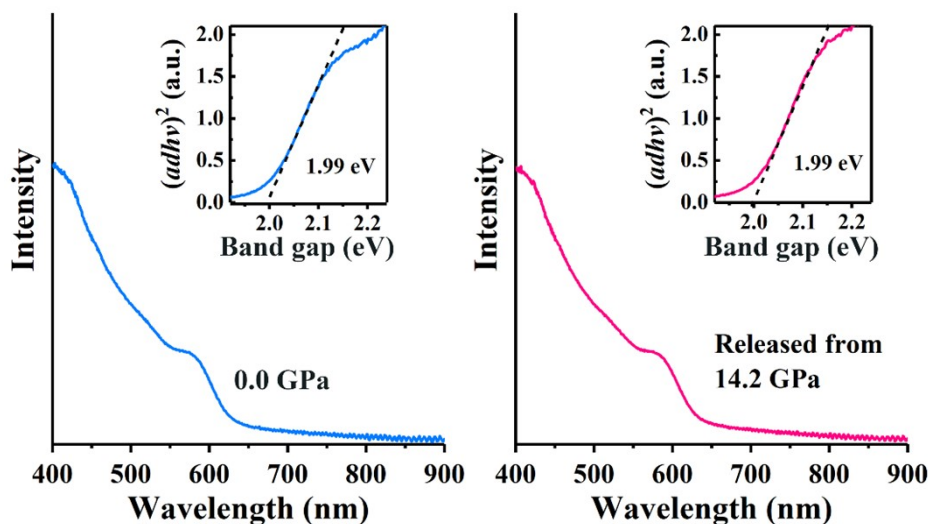


Figure S8 The absorption spectrum and band gap energy comparison of the InP/ZnSe NCs before and after ~ 14.2 GPa pressurization. Inset: Direct band gap Tauc plot of the InP/ZnSe NCs collected at 0 GPa and 14.2 GPa, respectively. After a compression cycle of 0–14.2 GPa, the absorption spectrum and band gap energy returned to its initial state.

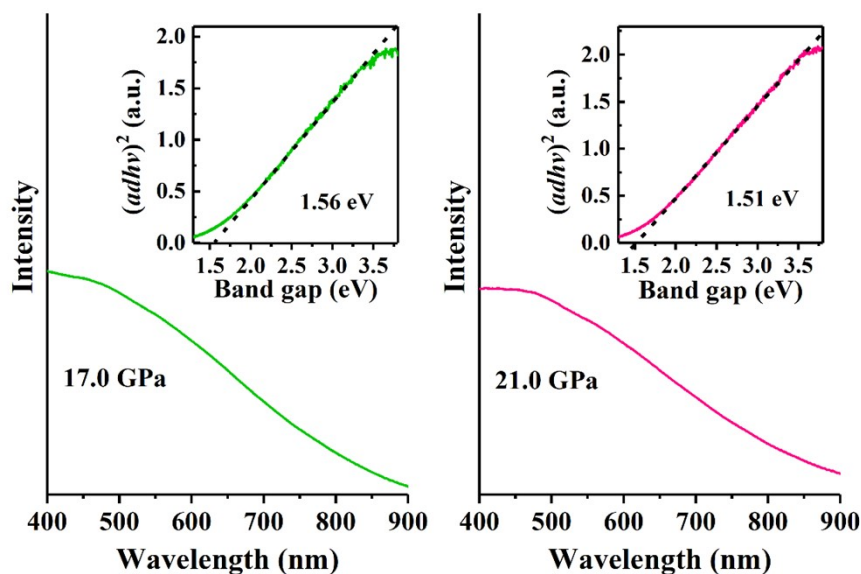


Figure S9 The absorption spectrum and band gap energy of the InP/ZnSe NCs at 17.0 GPa (left) and 21.0 GPa (right), respectively. Inset: corresponding direct band gap Tauc plot of the InP/ZnSe NCs.

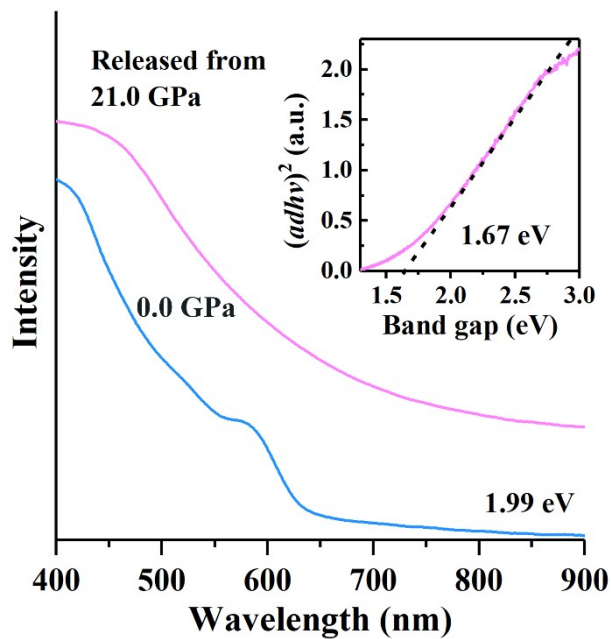


Figure S10 The absorption spectrum and band gap energy comparison of the InP/ZnSe NCs before and after ~21.0 GPa pressurization. Inset: Direct band gap Tauc plot of the InP/ZnSe NCs collected at 21.0 GPa. After a compression cycle of 0–21.0 GPa, the absorption spectrum and band gap energy show a red-shift compared to the initial that.

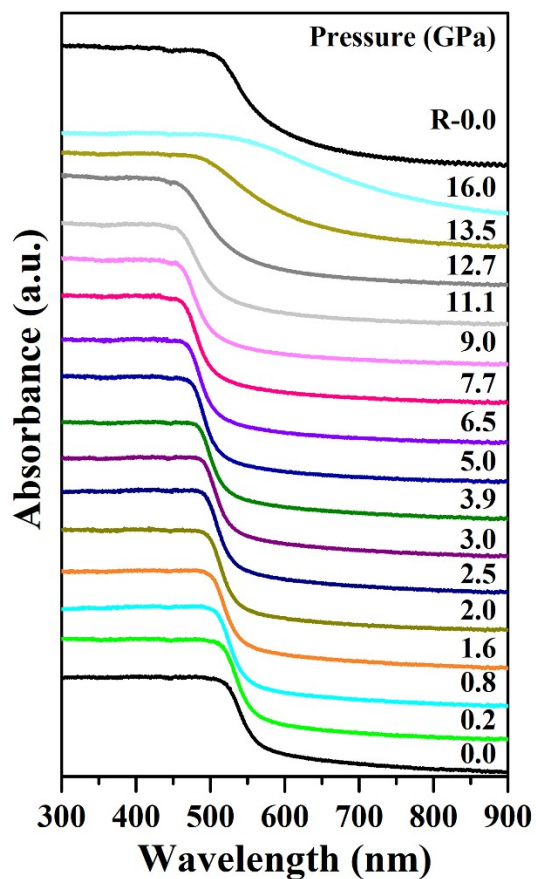


Figure S11 Absorption spectrum of the InP NCs as a function of the pressure.

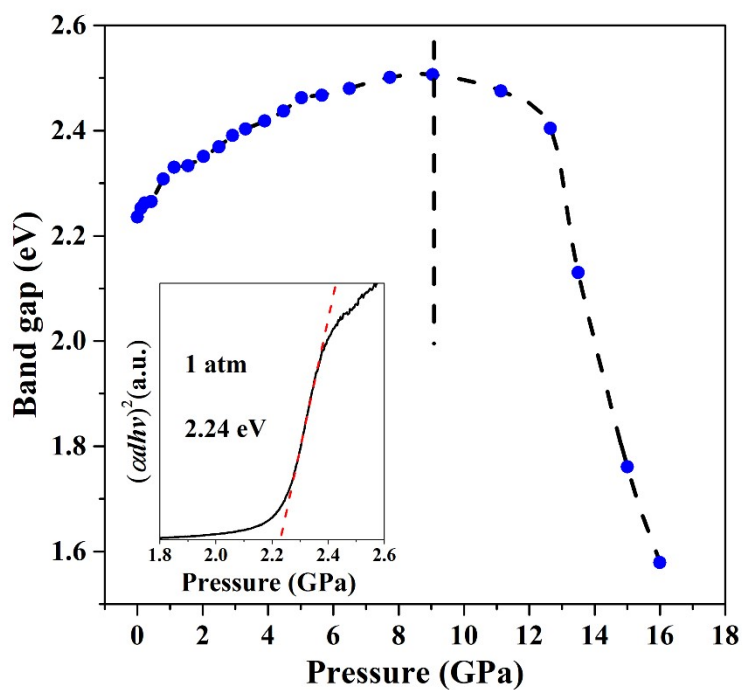


Figure S12 Shift of the bandgap energy of the InP NCs with pressure. Inset shows the Tauc plot of the InP NCs under ambient conditions.

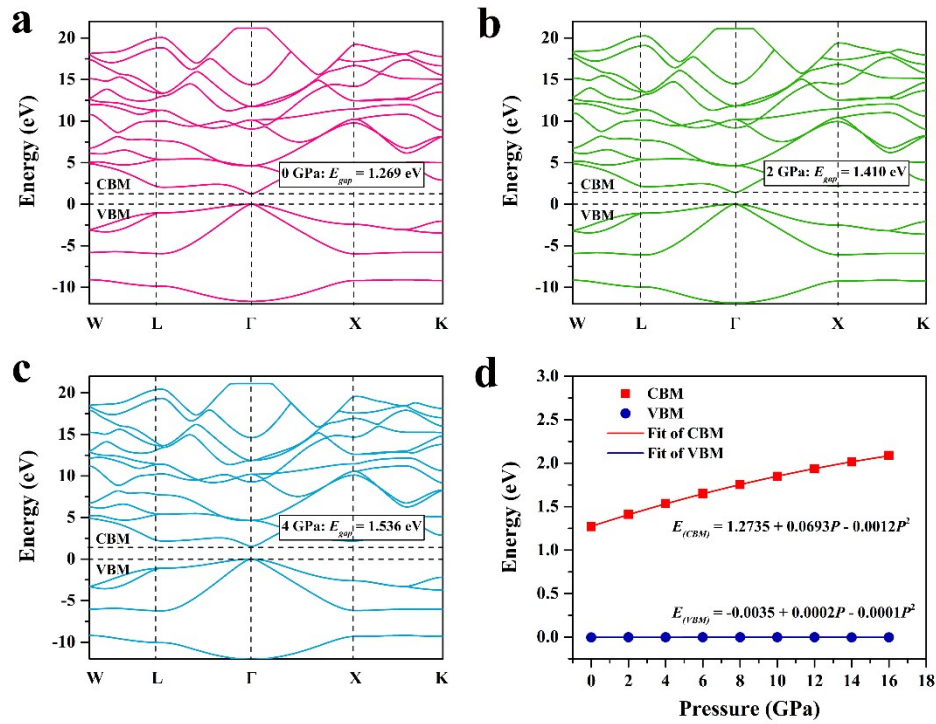


Figure S13 Energy band of InP at different pressures, (a) 0 GPa; (b) 2 GPa; (c) 4 GPa. (d) Energy of conduction band minimum (CBM) and valence band maximum (VBM) of InP with increasing pressure.

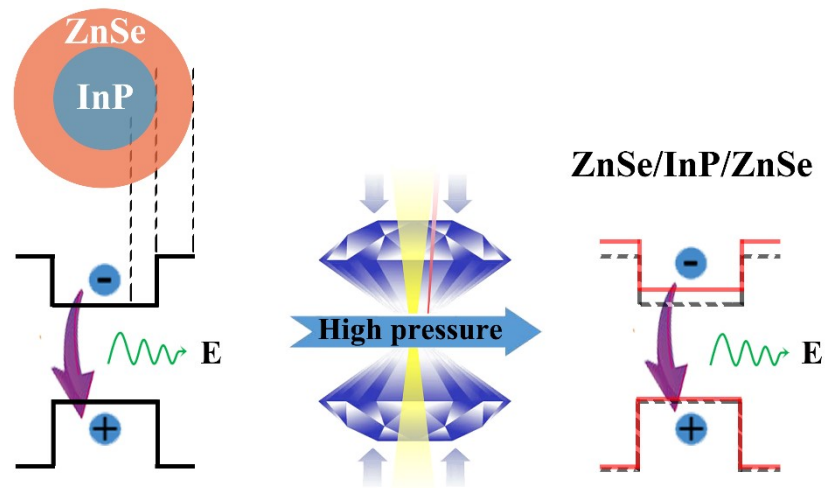


Figure S14 Schematic illustration of electronic energy levels for InP/ZnSe core/shell NCs at ambient conditions (left) and high pressure (right). The red lines depict the the changed energy levels under pressure, and dashed lines are the intrinsic band alignments.

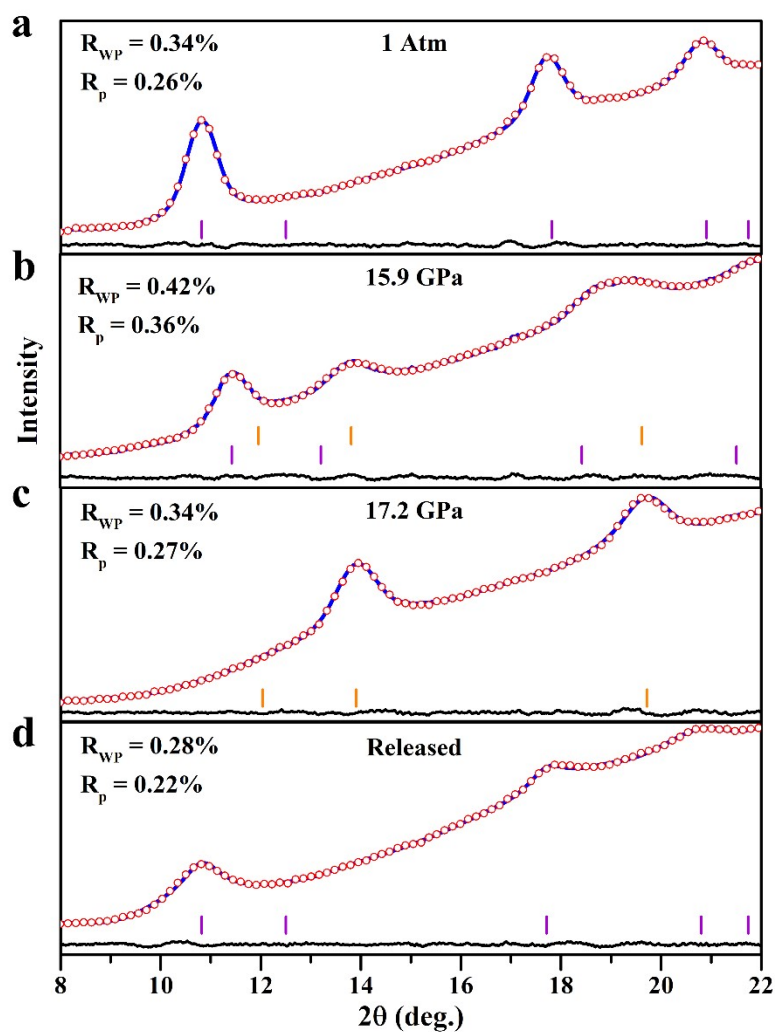


Figure S15 Rietveld refinements of the experimental (blue line), simulated (red circles), and difference (black line) ADXRD patterns of ZB structure at 0 GPa (a), mixed-structures at 15.9 GPa (b), RS structure at the pressure of 17.2 GPa (c), and ZB structure acquired after releasing the pressure from 21.5 GPa (d). Purple and orange vertical markers indicate the corresponding Bragg reflections of ZB and RS structure, respectively.

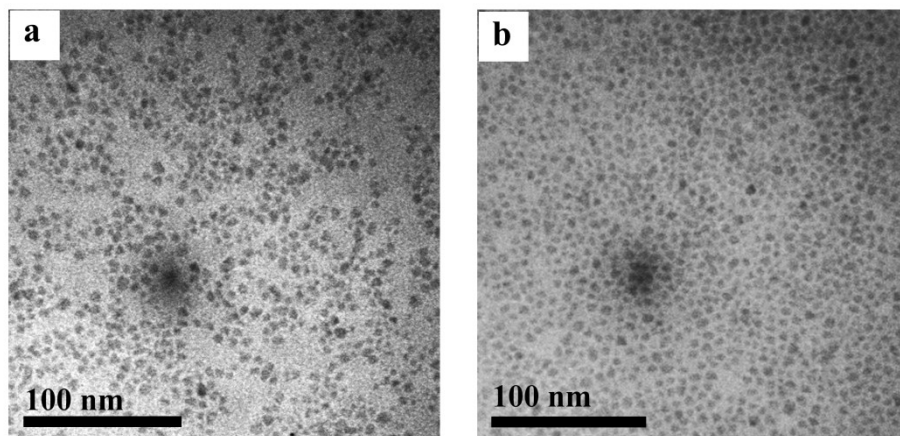


Figure S16 (a) Representative TEM image of the InP/ZnSe NCs, acquired after releasing the pressure from about 9.0 GPa. (b) Representative TEM image of the InP/ZnSe NCs, acquired after releasing the pressure from about 14.0 GPa.

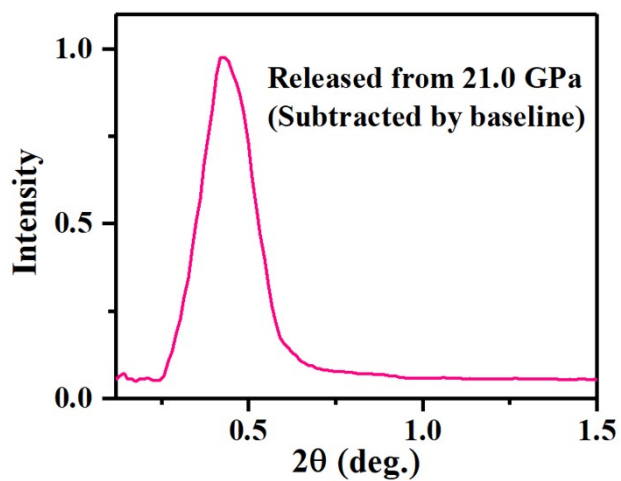


Figure S17 The SAXS spectrum (first SAXS peak) of post-compression samples was subtracted by baseline.

Table S1 The PLQYs of InP/ZnSe NCs under different pressure.

Pressure (GPa)	PL integral intensity I/I_0	Cell volume V/V_0	Refractive index square n^2	PLQY
0.0	1.000	1.000	20.151	30.09
0.6	0.836	0.992	21.408	26.72
1.7	0.616	0.979	23.727	21.83
2.5	0.524	0.970	25.793	20.18
3.5	0.417	0.958	28.778	17.92
6.6	0.192	0.924	45.118	12.94
7.7	0.139	0.911	57.604	11.96